An Experimental Study On The Aerodynamic Performance Of A Novel Laminar-Flow-Enabling Snap-Fit Seal

Harry Ramsay*, Alden Midmer† and Chetan Jagadeesh‡
City, University of London, London, EC1V 0HB

Anthony Finnerty §
University of Oxford, Oxford, OX1 2JD

Tim Evans¶ and Chris Vaissiere‖
Jigsaw Structures Ltd., Bristol, BS16 7FR

This work investigates the aerodynamic and pressure sealing performance of the ALFA seal, a novel fixed-leading-edge to main wing-box seal that is designed to maintain laminar flow over the leading edge of a transonic wing. The seal also offers benefits beyond aerodynamics, by simplifying assembly and maintenance through its snap-fit design which eliminates the need for sealants and bonding applications. Wind tunnel experiments were conducted using Laser Doppler Anemometry (LDA) and Schlieren imaging to assess the seal's impact on the boundary layer and its pressure sealing capabilities. LDA measurements suggest minimal influence of the seal on the flow velocity profile, with consistent turbulence intensity across various Mach numbers. Schlieren visualizations revealed flow disturbances originating from the seal's leading edge, potentially impacting the downstream flow. This discrepancy highlights the need for further investigation using an extended LDA measurement range and single-plane focused Schlieren imaging techniques. Pressure sealing tests demonstrated the seal's ability to maintain pressure differentials across the wing, replicating those experienced during flight. Overall, the results are promising for the ALFA seal's potential as a laminar flow enabler and sealing device for commercial aircraft wings. Further investigation are necessary to fully understand its impact on the boundary layer and optimize its design.

I. Introduction

Minimizing aerodynamic drag is a critical factor in reducing the environmental impact of the aviation sector, specifically its carbon footprint. The wing of the future will focus on the reduction of lift-induced drag KC_l^2, and will achieve this in two primary ways; the aspect-ratio AR of wings will continue to increase resulting in longer, more slender wings and, of particular focus in this study, very low zero-lift drag C_{D0} values will be sought after. While much of the work in reducing emissions has been done by the recent advances in jet propulsion, gains in efficiency are still to be made in the performance of aerodynamic surfaces, the most obvious of which is the wing. The ability to maintain laminar flow over a large section of wing could lead to the saving of millions of liters of fuel per year throughout the industry [1] and a consequent reduction in greenhouse gas emissions and operational costs. Excrescence drag amounts to approximately 7% of total drag of a typical single-aisle aircraft [2], of which approximately 2.5% can be attributed to surface irregularities due to gaps and mismatches. Using the fixed-trade calculator developed by the Aerospace Technology Institute (ATI), it is estimated that reduction of 2.5% drag amounts to a decrease in block fuel burn cost per aircraft per year of $180,000, along with a decrease in carbon dioxide emitted per aircraft per year by approximately 460,000 kg. This tool presupposes that the reference aircraft is a narrow body representative of year 2000 Entry Into Service technology levels, with a utilization of more than 1700 flights per year with an average leg of 750 NM.

Current wing assembly methods introduce gaps, steps and surface roughness into the airflow, leading to earlier transition to turbulent flow [3]. Holmes et al.[4] suggests fuel efficiency improvements of nearly 25% could be achieved

*Doctoral Researcher, School of Science and Technology, City, University of London
†Doctoral Researcher, School of Science and Technology, City, University of London
‡Senior Lecturer in Aeronautics, School of Science and Technology, City, University of London
§Doctoral Researcher, Oxford Thermofluids Institute, University of Oxford
¶Director, Jigsaw Structures Ltd
‖Director, Jigsaw Structures Ltd

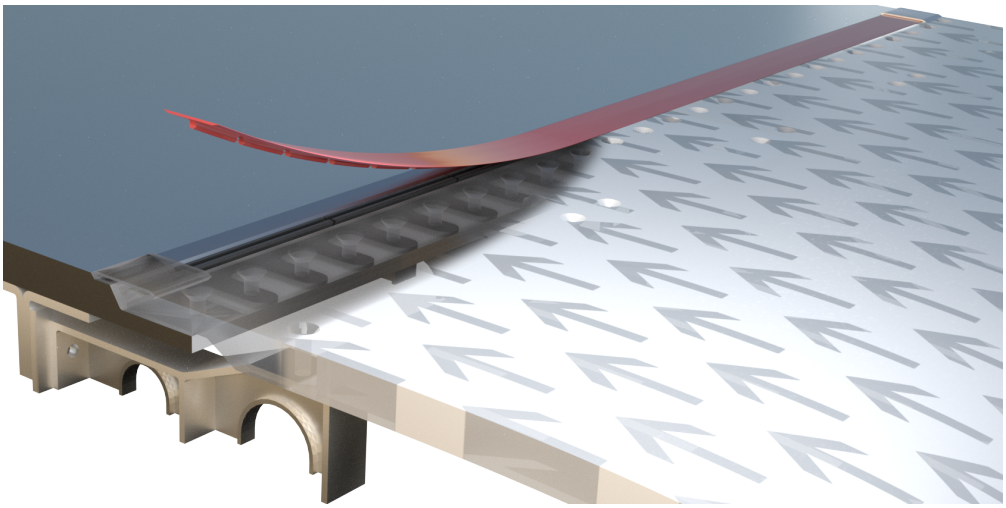

Fig. 1 Example application of the seal within the leading edge of a typical single aisle passenger aircraft. The flexible seal is shown being installed into a wing section with flow from right to left.

through the development of methods of maintaining laminar flow across surface discontinuities such as those between a fixed leading edge and main wing body. It is this specific discontinuity in the surface, shown in figure 2, that this project investigates though the final product has applications on other external aerodynamic surfaces where gaps are present. Holmes et al.[4] also defines a number of manufacture and assembly criteria for maintaining laminar flow - some of which are the removal of steps, gaps and the reduction of surface roughness, these criteria are met by the ALFA-Seal (Advanced Laminar-Flow Enabling Seal, Patent no. GB2545153) investigated herein.

II. Background, ALFA-Seal

In addition to the improvement in aerodynamic performance intended by the design, the seal has additional benefits in the assembly and maintenance stages of aircraft life. The snap-fit installation method is ideal for automated assembly and removes the need for sealant application and curing time. This would contribute to a decrease in assembly time and the subsequent increase in aero-structure production rates [5]. Removal of the seal compared to typical sealants is also far simplified, with a single, sacrificial piece to be removed rather than the time-consuming removal process of a bonded sealant. ALFA-Seal is new technology designed to be incorporated into the next generation natural laminar flow wing. It therefore can't be retrofitted into the wing gaps on pre-existing aircraft.

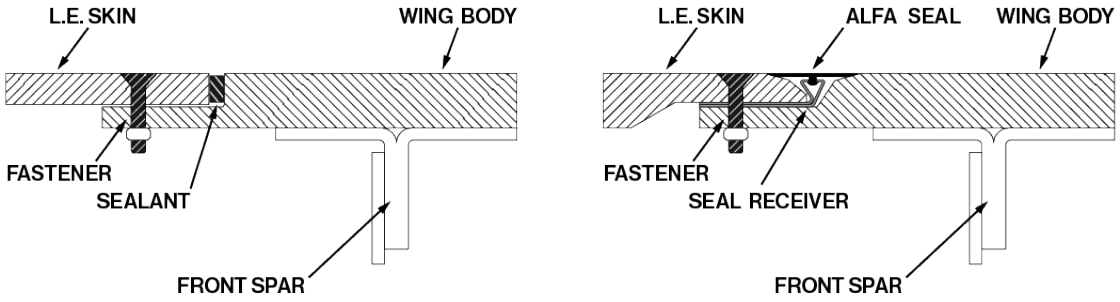

Fig. 2 Diagram of the typical wing assembly method (left) (modified from [6]) and the proposed ALFA seal solution (right).

The seal takes form of a disposable snap-fit component and a receiving channel to be manufactured as part of the

wing structure. Figure 1 shows an example installation of the seal for a typical leading edge construction. The right of the image presents the leading edge section of the wing, with the joint to the main wing body, left side, covered by the ALFA seal. A number of designs have been generated in different forms, with some offering the ability to conceal fasteners as well as sealing gaps. The application shown in Fig. 1 is more complex than the experimental model used section III, though the appearance and geometry at the surface remain the same.

Investigations on the impact of the seal on the boundary layer across a tunnel liner mimicking the leading edge section of a transonic airfoil are carried out using the National Wind Tunnel Facility's transonic wind tunnel at City, University of London. Both qualitative and quantitative data is recorded using Schlieren imaging and laser Doppler anemometry (LDA) to perform comparative studies between upstream and downstream flow.

III. Experimental arrangement and methods

Experiments were carried out at a range of Mach numbers relevant to single isle commercial aircraft - Mach 0.5 to Mach 0.9. Qualitative data was acquired through Schlieren imaging in a Z-type configuration, Fig. 3, consisting of two 8-inch diameter parabolic mirrors with a 6ft focal length, a high-power LED point light source, and a Phantom Miro 310 high-speed camera. The camera is capable of frame rates up to 40 000 frames-per-second with the required capture area [7].

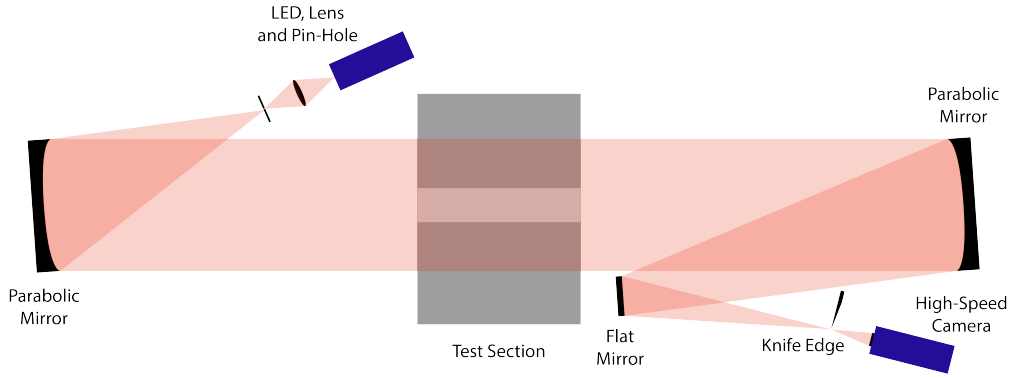

Fig. 3 Z-Type Schlieren imaging setup around the transonic tunnel test section.

Quantitative data for the boundary layer velocity profile was acquired using a laser Doppler anemometry setup from Dantec Dynamics. The FiberFlow system is mounted on a 3-axis traverse position around the test section. This allows for fast and automated collection of velocity data at a range of wall distances.

The test section was equipped with a custom liner, Fig. 4, that allows the integration of the seal into the floor of the tunnel, and also the ability to apply a pre-load on the seal to hold it against the surface. The receiving channel runs on a linear guide rail and can be moved through the use of two stepper motors. This downwards force on the seal keeps it seated against the wall and resists the suction forces formed by the flow over the surface.

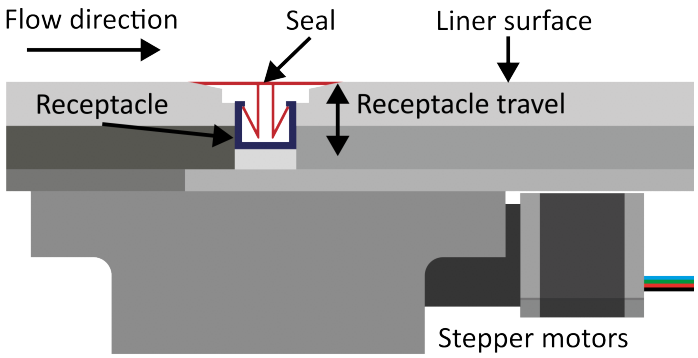

Fig. 4 Custom test-section liner showing the seal receiving channel and flow surface.

Early shakedown testing showed the magnitude of these suction forces were capable of warping the test section itself between it's fixings at either end of the section. This was eliminated through additional strengthening and securing the liner in the center of the section.

A. Mechanical Properties

In order to apply a known force to the seal through the stepper motors, a test scheme was carried out to find the force-displacement relationship. Once in place in the test section, the known displacement of the receptacle can be translated into the applied loading force. Testing was conducted with a custom test rig in an Instron Universal Testing System. The system can apply a maximum load of 50 kN at a speed of $0.001\,\mathrm{mm\,min^{-1}}$.

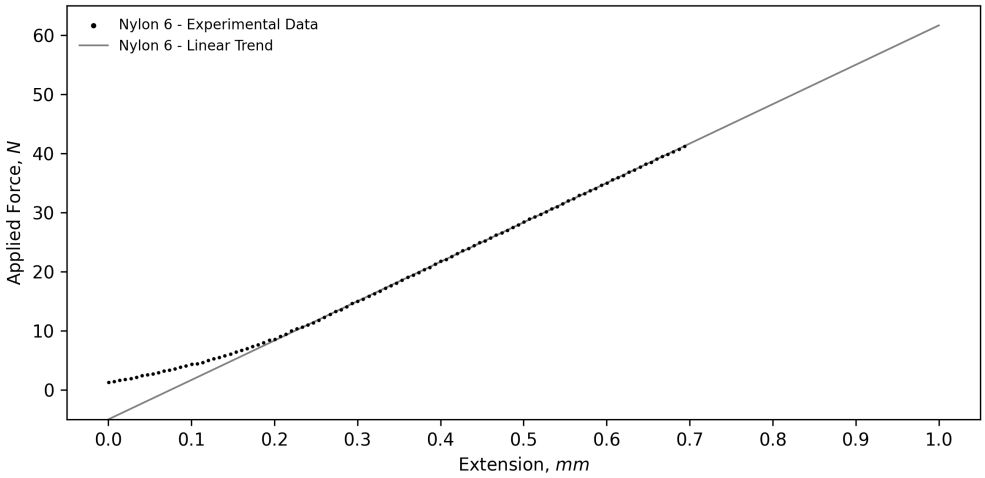

Fig. 5 Force-Displacement relationship from mechanical testing.

Figure 5 shows the results of this testing and highlights how care should be taken when using this data during tunnel testing. The non-linear region at the beginning of the tests is due to the displacement measurement not reading zero exactly at the point where the seal is flat and seated against the walls. During testing, a procedure was established such that the displacement measurement could be accurately zeroed and the applied force calculated correctly using the linear relationship. The linear relationships found through mechanical testing matched closely with simulations undertaken by the projects industrial partner, Jigsaw Structures Ltd.

B. Electronic Pre-Loading

As mentioned, a pre-load force can be applied to the seal component such that it remains in contact with the liner surface through the high-speed test runs. This is done through the use of two counter-rotating stepper motors and gearboxes. The reduction gearbox allowed for a vertical movement of the seal of approximately 0.14 mm per 100 motor steps. Before a test, a mechanical clock depth gauge is used to measure the displacement and subsequently, the applied pre-load. During testing, a laser displacement sensor is installed on the exterior of the tunnel (Fig. 6) to measure the movement of the seal.

C. Laser Doppler Anemometry

Two component boundary layer profile information is collected using a single, two-component probe with lasers of 488 nm and 514 nm. Transmitting optics are mounted at 45° to the liner surface with velocity data transformed to provide stream-wise and wall-normal flow components. The scattered light from the particles passing through the probe volume contains a Doppler Shift, with the Doppler Frequency, f_D, providing the time component for the velocity calculation [8]. The distance component comes from the fringe spacing, d_f, resulting from the interference between the split laser beams. Signals collected through the receiving optics are processed using Dantec Dynamics Burst Spectrum Analyzer (BSA).

The optics were positioned using the traverse to take measurements between 0 mm and 15 mm above the surface at

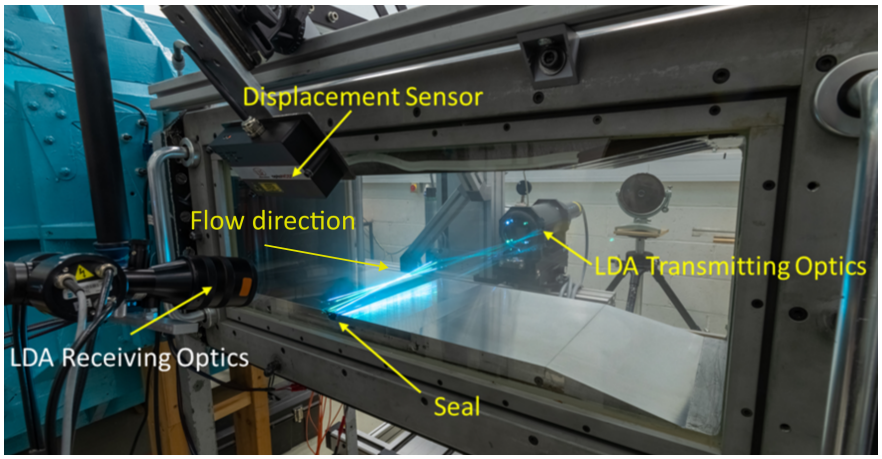

Fig. 6 LDA Setup through test section centerline.

locations upstream, downstream and on the seal itself, Fig. 6.

D. Initial Test Matrix

To gain an initial understanding of the aerodynamic performance, experiments were carried out at a range of Mach numbers. In each case, measurements were first taken upstream of the the seal in order to determine the state of the unaltered flow. Measurements were then made upon the seal and downstream of the seal, which were compared to the upstream measurement to determine the impact of the seal on the flow. Targeting narrow body commercial aircraft in the transonic regime, tests were conducted at Mach 0.3, 0.5, 0.7 and 0.9. These tests covered in the scope of this report were all completed at a single pre-load of 200 N which was determined to maintain the required differential pressure at all operating Mach numbers (see Fig. 14).

IV. Results

A. Initial Test Profiles

This included ensuring the Burst Spectrum Analyzer software was targeting the correct flow speeds for each Mach number and that a suitable number of data points were interrogated within each test configuration. Also setup were the measurement stop conditions which trigger the movement of the traverse onto the next grid point. Stop conditions of ten-thousand samples or five seconds of data recording were found to provide good levels of data for most points whilst ensuring that all points can be attempted during a single run.

Both upstream and downstream locations were set at ±50 mm from the center of the seal to compare the affect on the flow. The initial upstream velocity profile at Mach 0.3 can be seen in Fig.7. From this and the other initial profiles, it was decided to increase the resolution of the measurements around the edge of the boundary layer as well as in the free-stream. These points were easily added as there is a sufficiently high data-rate (approx. 10 000 Hz) at this wall distance to not impact the runtime of the test.

B. Resulting LDA Velocity Profiles

Following the previously mentioned test matrix, twelve tests were completed. Figure 8 shows the resulting mean velocity profiles as a product of free-stream velocity. Shown for each Mach number are the velocity profiles before, on, and after the seal. With majority of data points recording 10 000 samples, the mean u velocity is plot along with the 10th and 90th percentile. This provides a quick indication to the possible turbulence level at each location. On initial glance, the velocity distributions look very similar, suggesting the seal has little effect on the flow. The range spanning 80% of the samples also looks similar between each stream-wise location, suggesting the turbulence level is similar. This can be seen more closely by considering the histogram of the recorded data for a particular wall-distance and Mach number. Figure 9 shows the resulting histograms for the data recorded at Mach 0.5 at a wall normal distance of 1 mm.

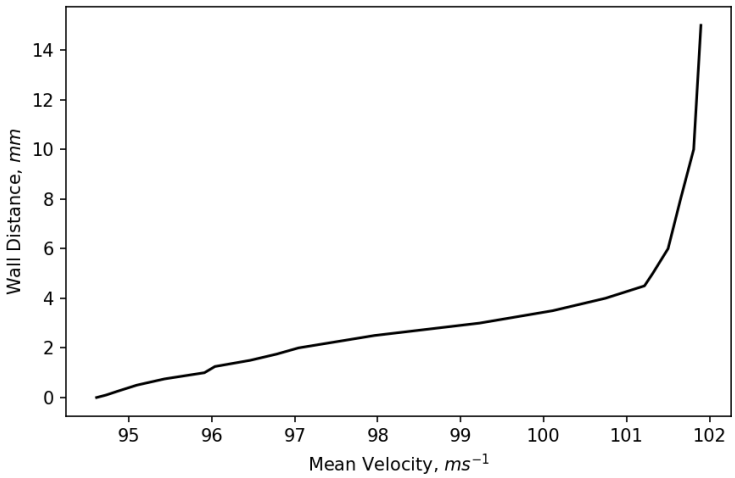

Fig. 7 Initial velocity profile at Mach 0.3, upstream of the seal location.

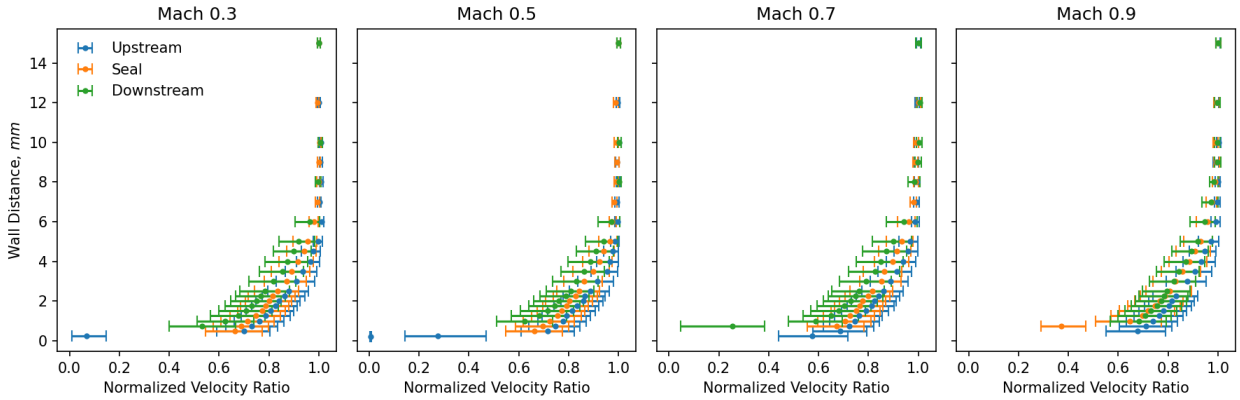

Fig. 8 Velocity profiles for each test case showing the mean velocity and 10th and 90th percentiles.

It can be seen in each of these cases that the span of velocity measurements is very similar, with 80% of the data on average spanning 20% of the free-stream velocity.

For a better understanding of the flow turbulence, the turbulence intensity, T, can be found. From [9]

$$T = \frac{\sqrt{\frac{1}{3}\left(\overline{u'^2} + \overline{v'^2} + \overline{w'^2}\right)}}{U_\infty} \tag{1}$$

In most wind tunnel test environments, and assumed in this test case due to the magnitude difference between the stream-wise and wall-normal velocities, the turbulence intensity can be written simply as

$$T = \frac{\sqrt{\overline{u'^2}}}{U_\infty} \tag{2}$$

Calculating the turbulence intensity for each measurement location results in Fig. 10. From this plot, it can be clearly seen for all free-stream velocities that the turbulence intensity increases after the leading edge of the seal. Between Mach 0.3 and 0.7, turbulence intensity increases by approximately 14 % at the seal center, and by 34 % after the seal. At Mach 0.9, the turbulence intensity after the seal remains much the same as on the seal itself, suggesting at this point the affect of the leading edge of the seal is great enough that the trailing edge makes no discernible difference.

When comparing the turbulence intensity at a single location across the Mach range, it appears in most cases that the free-stream velocity does not impact the turbulence intensity downstream of the seal. This is with the exception of when

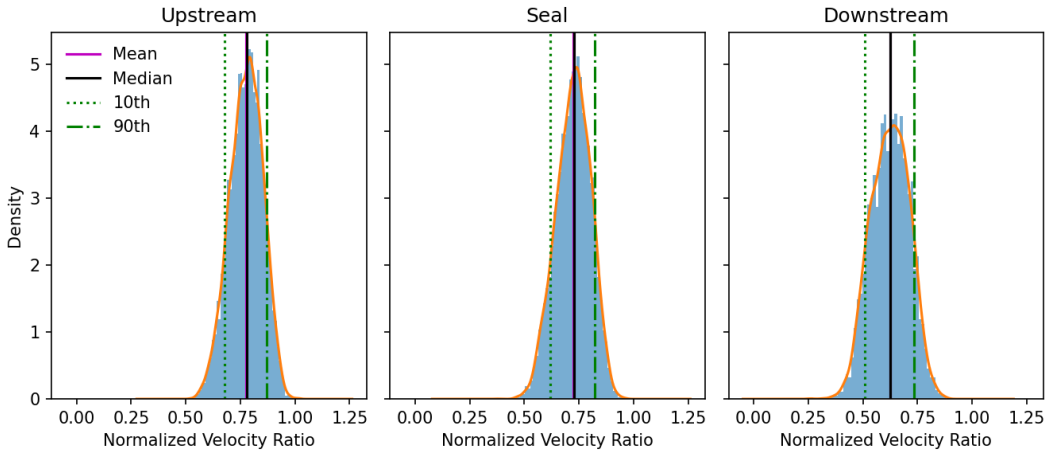

Fig. 9 Histograms of data points at Mach 0.5, 1 mm from the wall at each stream-wise position.

the flow reaches Mach 0.9. This matches an observation made by [6] which found the location of transition triggered by a surface gap was not dependent on Mach number, until the flow reached Mach 0.9. Similar to this study however, it could not be concluded that this is due to the change in Mach number as the Reynolds number is not constant. A case wherein the free-stream velocity does not affect the final downstream turbulence intensity is advantageous however, as it allows for a single optimized seal setup to be used across the entire operating range, without any need to manipulate or change the seal setup during flight.

The analysis of velocity profiles provides valuable quantitative data, but uncertainties remain regarding the overall flow structure. Repeating these measurements and incorporating Schlieren imaging can help address these uncertainties. Schlieren visualizations, when analyzed alongside the velocity profile data, can highlight potential inconsistencies in the measurements and offer insights into the flow behavior. This combined approach can lead to a more comprehensive understanding of the flow characteristics around the seal.

C. Schlieren Imaging

Schlieren imaging was carried out across the same Mach number range with the same single seal configuration. The resulting time-averaged flow can be seen in Fig. 11. The locations of the three LDA measurement locations are also highlighted on these images. Looking at the Mach 0.9 case, Fig. 11c, as this shows the largest contrast, the boundary layer can be seen to extend to approximately 8 mm from the wall at the downstream location. This is calculated using the seal width as a reference dimension. Similarly, the numerical data in Fig. 8 suggests a boundary layer thickness of 8 mm also.

High-speed video footage revealed flow disturbances originating at the leading edge of the ALFA seal and expanding downstream. This transient flow phenomenon is not evident in time-averaged images but exhibits clear turbulent-characteristics. Notably, at the downstream location of the LDA measurements, this disturbed flow region extends beyond the farthest point measured from the wind tunnel wall.

The absence of this characteristic in the downstream LDA data suggests a potential dimensionality-difference between the laser-based measurement technique and the Schlieren imaging [10]. While Schlieren visualizes the flow across the entire tunnel width, the LDA measurements provide data only for a central two-dimensional cross-section. This discrepancy highlights the possibility of three-dimensional flow structures influencing the Schlieren observations but not captured by the point-wise LDA measurements. The seal used during these runs did not span the entire width of the tunnel, leaving a gap at each side. It is highly likely that the turbulent flow seen in the Schlieren imaging growing from the the start of the seal slow is actually found at the tunnel wall and not being formed as a results of the seal itself.

Also seen as a result of the gaps present at each end of the seal is a leakage flow from the cavity beneath the surface of the test rig. The next round of testing solved these issues by sealing the gaps between the seal ends and the tunnel wall and ensuring that the flow is as uniform as possible across the span of the test section, giving the most accurate 2D representation of the flow.

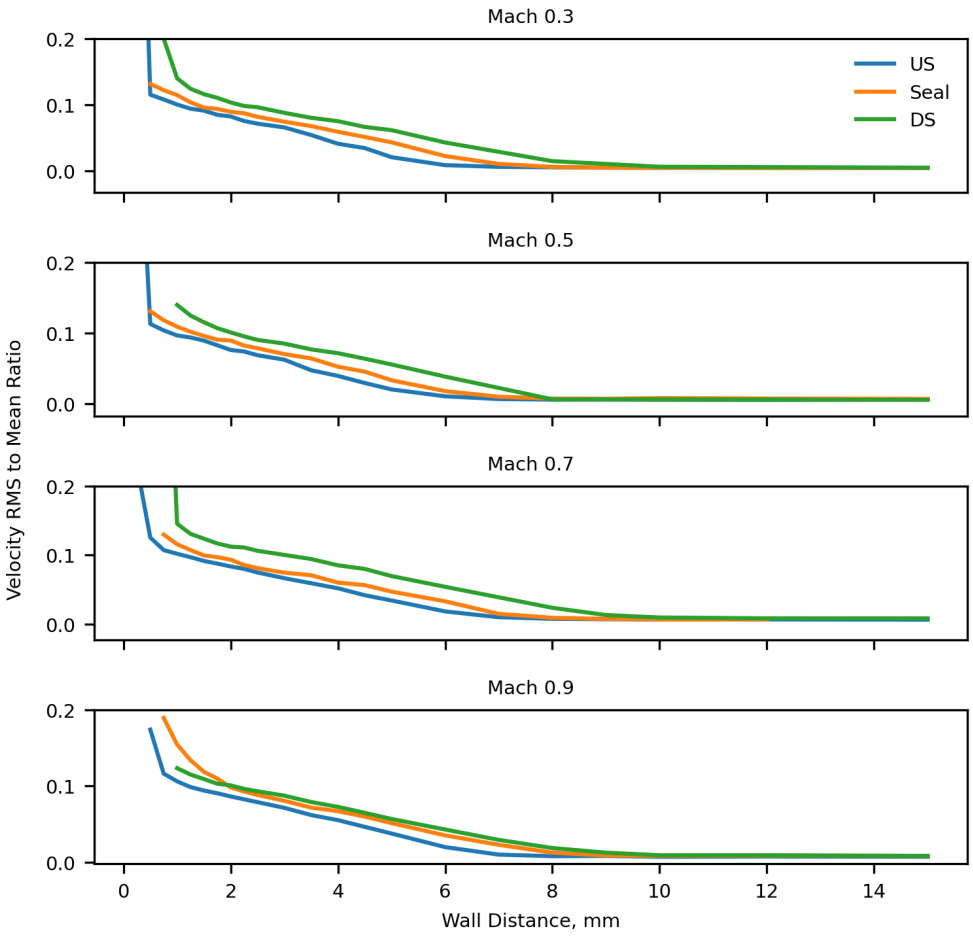

Fig. 10 Turbulence Intensity at each measurement location.

D. Pressure Sealing

In order to test the sealing capabilities of the seal, static pressure was measured at the tunnel wall and in the cavity beneath the seal- representative of the pressure difference between the pressure and suction side of the wing which the seal would have to hold. Running the tunnel at different Mach numbers would allow a different pressure difference between the two sides of the seal. A target theoretical pressure difference can be calculated given a flight altitude and Mach number using [11]

$$\Delta P = \Delta C_P \left(\frac{1}{2} \rho_{fl} \cdot \left(M_\infty \cdot a_{fl} \right)^2 \right) + P_{fl} \tag{3}$$

where ΔC_P is the difference in pressure coefficient between the upper and lower wing surface. With the desired pressure delta calculated, the data from the mechanical testing can provide the theoretical load required on the seal to withstand the suction force generated. Initial targets set by Jigsaw Structures for an ultimate, cruise and limit differential pressure were found to require the tunnel be run at Mach 0.4, 0.6 and 0.8.

Figure 12 shows the potential outputs at Mach 0.8 for different seal loading amounts. With 0.14 mm of displacement, the seal does not provide a pressure tight seal and as such the pressure in the void beneath the seal begins to equalize with the tunnel static pressure. Although the seal does not allow complete pressure loss the pressure delta is below what is required. A further 0.14 mm of displacement brings the pressure delta much closer to what is required at 25 kPa. Due to the nature of the testing equipment and with the tunnel not being designed to maintain a pressure seal between the underside of the liner and the flow section, a complete seal is not completely achievable. It was decided that a complete seal could be said to be achieved when changing the displacement of the seal no-longer changed the pressure delta across the seal. This can be seen in Fig. 13 when the seal displacement exceeds 0.19 mm.

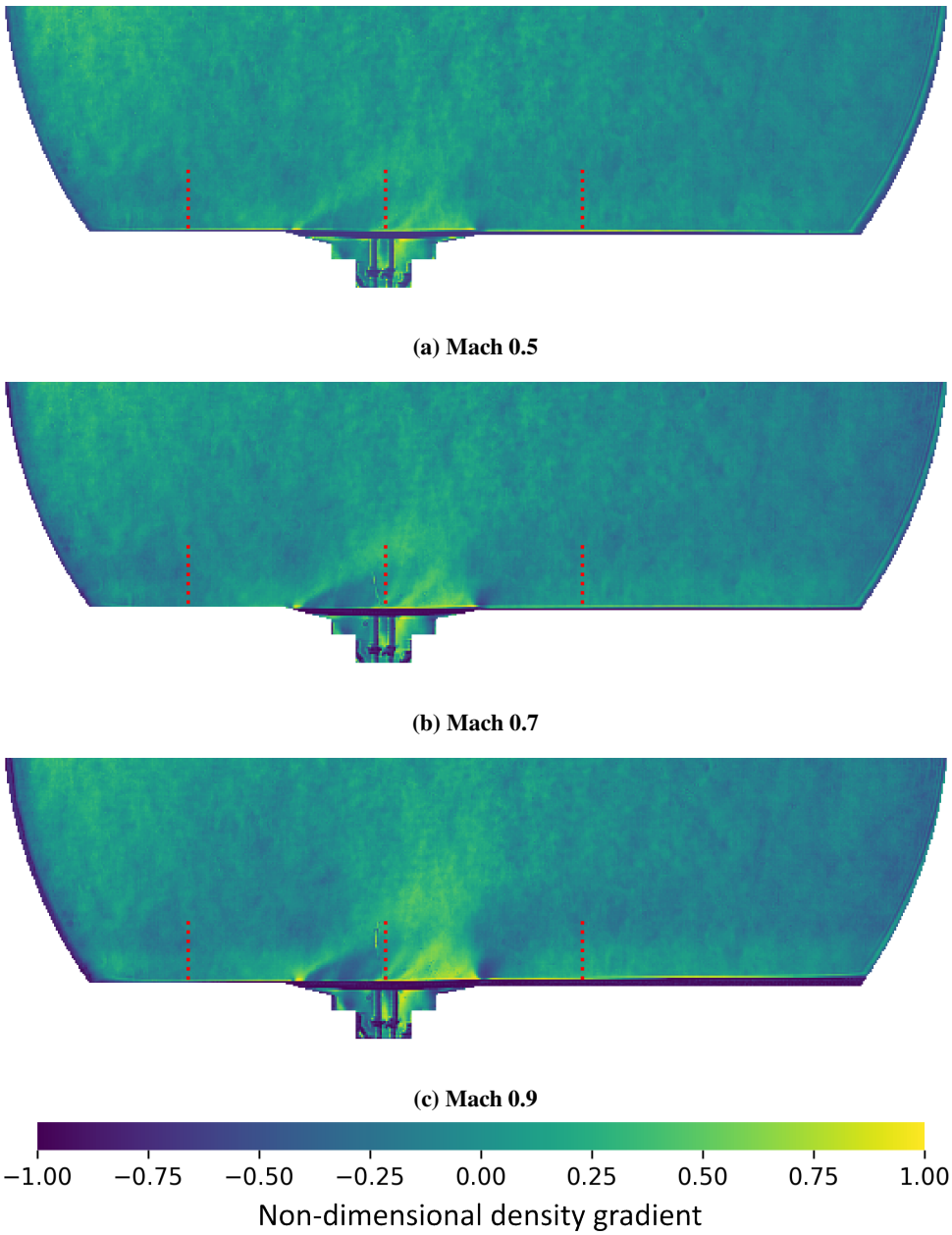

Fig. 11 Schlieren imaging of flow over seal. Flow from left to right. Dashed lines represent LDA measurement location.

Considering directly the applied pre-load force against the pressure delta experienced, this excess force applied for a complete seal can be seen more clearly. Figure 14 shows how in each case after a particular force is applied the sealing characteristic does not change and any additional pre-load may just lead to excessive wear on the specimen.

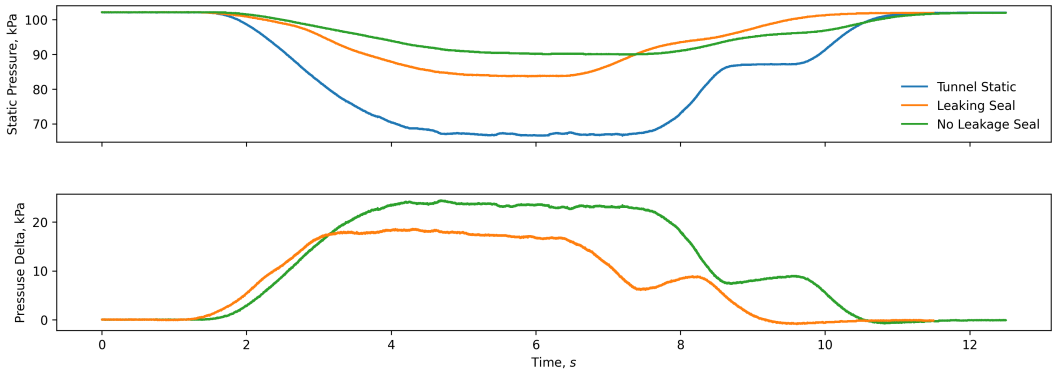

Fig. 12 Static pressure measurements between the tunnel and the underside of the seal showing a leaking and properly situated seal.

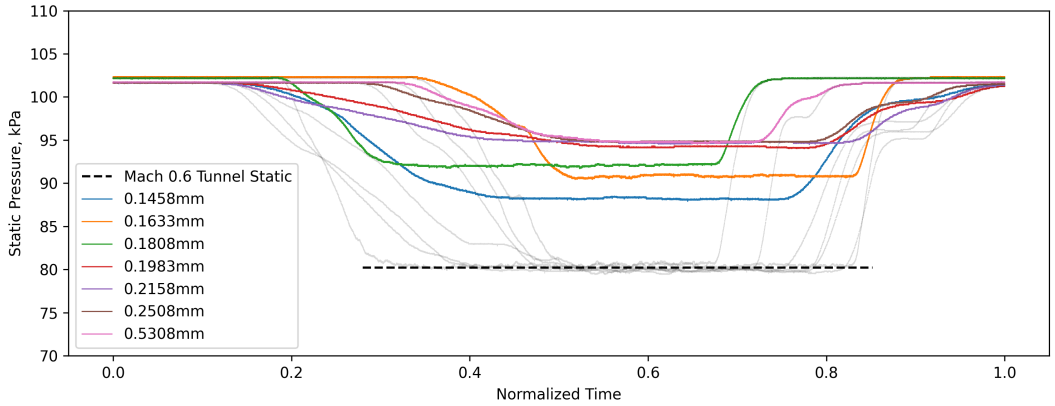

Fig. 13 Pressure delta across the seal with different pre-load displacements at Mach 0.6**.**

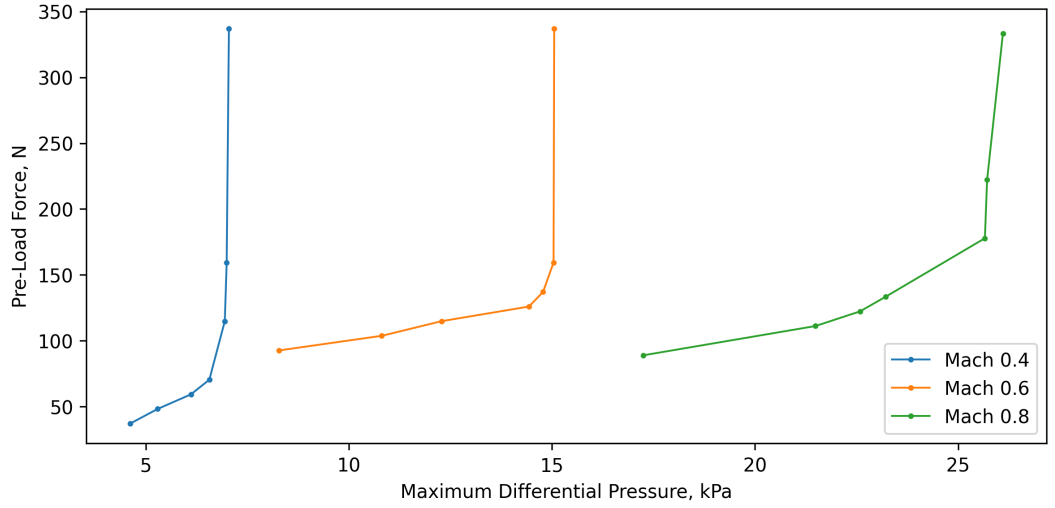

Fig. 14 Applied pre-load force required for a given maximum pressure delta.

V. Conclusion

Laser Doppler Anemometry (LDA) has been used to measure velocity profiles at three locations around the seal and Schlieren imaging has provided a corroborative, qualitative visualization of the flow. The LDA measurements suggest minimal impact on the flow from the seal itself, with similar turbulence intensity observed across the tested Mach numbers. However, Schlieren imaging revealed flow disturbances originating from the leading edge of the seal which extend downstream. This discrepancy highlights potential areas that need further investigation with LDA, namely an extended measurement range further into the free-stream. For the Schlieren imaging itself, single-plane focused Schlieren, such as that described in [12], would also allow for the data to be recorded at the tunnel centerline only, and as such provide a greater correlation with the LDA measurements. The LDA traverse also has the capability to be setup in a scanning method, where the data is recorded continuously as the traverse moves rather than stopping and recording discrete data points. This could also be beneficial as it would greatly increase the resolution of the data without requiring a longer tunnel run-time.

To assess the seal's capability of maintaining pressure differentials across the wing, dedicated pressure sealing tests were also conducted. These tests aimed to replicate the pressure differentials experienced by a transonic wing during flight by subjecting the seal to comparable pressure gradients across the suction and pressure sides.

As a proof-of-concept, the current results are promising regarding the sealing properties and demonstrate good potential for use as a sealing device on commercial aircraft.

Acknowledgments

The authors would like to acknowledge support from InnovateUK via the National Aerospace Technology Exploitation Programme (NATEP), under grant numbers 99852 and 10063728.

References

[1] Anderson, D., "Fuel Conservation: Airframe maintenance for environmental performance." , 2006.

[2] Goldhammer, M. I., and Plendl, B. R., "Surface coatings and drag reduction," *Aero Magazine*, 2013.

[3] Drake, A., Bender, A., Korntheuer, A., Westphal, R., Rohe, W., Dale, G., McKeon, B., and Geraschchenko, S., "Step excrescence effects for manufacturing tolerances on laminar flow wings," *48th AIAA Aerospace Sciences Meeting Including the New Horizons Forum and Aerospace Exposition*, 2010, p. 375.

[4] Holmes, B. J., Obara, C. J., and Martin, G. L., "Manufacturing Tolerances for Natural Laminar Flow Airframe Surfaces," *Domack Source: SAE Transactions*, Vol. 94, 1985, pp. 522–531. URL `https://www.jstor.org/stable/44729695`.

[5] ALFA-Seal, "ALFA Seal Project Summary – Public," , 2021. URL `https://www.alfaseal.org/wp-content/uploads/2021/04/ALFA-Seal-Project-PUBLIC.pdf`.

[6] Drake, A., Westphal, R. V., Zuniga, F. A., Kennelly Jr, R. A., and Koga, D. J., "Wing leading edge joint laminar flow tests," Tech. rep., 1996.

[7] Phantom, *Phantom Miro LAB-,LC- and R-Series Cameras Data Sheet*, ????

[8] Adrian, R. J., "Laser velocimetry," *Fluid mechanics measurements*, Routledge, 2017, pp. 175–299.

[9] Schlichting, H., and Kestin, J., *Boundary-layer theory*, 7th ed., McGraw-Hill, London;New York;, 1979.

[10] Hargather, M. J., and Settles, G. S., "A comparison of three quantitative schlieren techniques," *Optics and Lasers in Engineering*, Vol. 50, No. 1, 2012, pp. 8–17.

[11] Von Mises, R., *Theory of Flight*, Dover Publications, Incorporated, Mineola, 1959.

[12] Kantrowitz, A., and Trimpi, R. L., "A Sharp-Focusing Schlieren System," *Journal of the Aeronautical Sciences*, Vol. 17, No. 5, 1950, pp. 311–314. https://doi.org/10.2514/8.1623, URL https://doi.org/10.2514/8.1623.